ELSEVIER

Journal of Molecular Catalysis A: Chemical 163 (2000) 147–156

JOURNAL OF MOLECULAR CATALYSIS A: CHEMICAL

www.elsevier.com/locate/molcata

Production of synthesis gas by steam- and CO_2-reforming of natural gas

G.F. Froment

Department of Chemical Engineering, Texas A & M University, College Station, TX 77843-3122, USA

Received 28 February 2000; accepted 22 June 2000

Abstract

The simulation of a steam/CO_2 reformer is based upon detailed intrinsic kinetics of reforming, including those of carbon deposition and -gasification. The internal diffusion limitations are accounted fot through the modeling. The influence of the steam/methane and the CO_2/methane ratio on the synthesis gas production and composition and on the net rate of carbon formation is illustrated.

Keywords: Synthesis gas; Steam- and CO_2-reforming (kinetics, coke formation, simulation)

1. Introduction

Natural gas mainly contains methane, but also ethane; propane, butane and even higher hydrocarbons. It is converted into H_2,CO and CO_2 on Ni, generally supported on alumina or by partial oxidation by air or oxygen/air mixtures. For the production of ammonia a synthesis gas with molar ratio of H_2/N_2 of 3 is needed and this is achieved in a secondary reformer that transforms the effluent of the primary reformer by means of air. If the syngas is to be used for methanol synthesis the $H_2-CO_2/CO+CO_2$ has to equal 2 and CO_2-reforming or partial oxidation may be considered. For oxo-synthesis the H_2/CO ratio should not exceed 1. General reviews on steam reforming have been written by Trimm [1], Bartholomew [2], Rostrup-Nielsen [3] and Twigg [4]. The present paper out1ines and discusses a fundamental approach for the kinetic modeling of nsyngas production and the application of these kinetic models to the simulation of steam- and CO_2-reforming.

E-mail address: gilbert.froment@skynet.be (G.F. Froment).

2. Intrinsic kinetics of steam- and CO_2-reforming of natural gas

Steam- and CO_2-reforming can be represented by the following globa1 reversible reactions, taking methane as an example:

$$CH_4 + H_2O = CO + 3H_2 \qquad r_1 \tag{1}$$

$$CO + H_2O = CO_2 + H_2 \qquad r_2 \tag{2}$$

$$CH_4 + 2H_2O = CO_2 + 4H_2 \qquad r_3 \tag{3}$$

The reactions (1) and (3) are endothermic, the water gas shift (2) is exothermic. The rates of disappearance of methane and the rate of formation of CO_2 are calculated from

$$R_{CH_4} = r_1 + r_2 \text{ and } R_{CO_2} = r_2 + r_3$$

Xu and Froment [5,6] and Vereecke and Froment [7] expressed the reforming scheme in a more detailed way, shown in Fig. 1 for a feed containing propane,

1381-1169/00/$ – see front matter
PII: S1381-1169(00)00407-6

Nomenclature

a_N	specific surface of Ni particle (M^2Ni/kg cat)
$c_{C,Ni,f}; c_{C,Ni;r}$	concentrations of carbon dissolved in nickel at the front and the rear of the Ni-particle (kmol C/m^3 Ni)d_p
d_p	particle diameter (m)
d_t	tube diameter (m)
D_i	Knudsen-, molecular- or effective diffusivity of component i (m^2/h)
g	acceleration of gravity (m/h^2)
ΔH	reaction enthalpy (kJ/kmol)
k_i	rate coefficient (kmol/kg cat. h bar^n); $n = -0.5$ for $i = 1, 3$; $n = 1$ for $i = 2$
K_i	adsorption equilibrium constant (bar^{-1})
p_i	partial pressure of i (bar) or (Pa)
p_t	total pressure (bar)
Q	$= U\Delta T$, heat flux from furnace to process gas (kJ/m^2 h)
rds	rate determining step
r_{CM}	rate of coke formation from methane cracking (kmol C /kg cat. h)
$r_{c,net}$	net rate of coke formation (kmol C /kg cat. h)
r_i	rate of reaction i (kmol/kg cat. h)
R	gas constant (kJ/kmol K)
R_p	particle radius (m)
T_i	absolute temperature (K)
x_i	conversion of component i
z	distance along reactor (m)

Greek symbols

η_j	effectiveness factor for reaction j
ρ_B	bulk density of the bed (kg cat/m^3 reactor)
ρ_S	particle density (kg cat/m^3 cat.)
ξ	dimensionless radial distance in catalyst particle
Ω	reactor cross section (m^2)

ethane and methane. The conversion of the hydrocarbon starts with 2 parallel dissociative adsorptions. Each of these adsorbed species further decomposes untill oxygen, generated from the dissociative adsorpion of steam, is inserted, yielding adsorbed CO. The latter is desorbed or transformed by an elementary step of the water gas shift into CO_2. The oxygen is inserted when the stage CH_2-1 is reached. Without this insertion the dehydrogenation of the adsorbed hydrocarbon radicals continues untill carbon is produced and deactivation of the catalyst starts (Fig. 2).

$$r_P = \frac{k_P^{+'} p_{C_3H_g}}{(DEN)^2},$$

$$r_E = \frac{k_E^{+'} p_{C_2H_6} - (p_{H_2}^{0.5}/p_{H_2}^{0.5} + \kappa) k_P^{+'} p_{C_3H_g}}{(DEN)^2},$$

$$r_M = \frac{k_M^{+'}(p_{CH_4} - (k_M^{-'}/k_M^{+'})\alpha_{CH_3-l} p_{H_2}^{0.5})}{(DEN)^2},$$

$$r_{CO} = \frac{(k_{CO}^{+'}/p_{H_2}^{2.5})(\alpha_{CH_3-l} p_{H_2}^{0.5} p_{H_2O} - (k_M^{+'}/k'_{CO} k_M^{-'}) p_{CO} p_{H_2}^3)}{(DEN)^2},$$

$$r_{CO_2} = \frac{(k_{CO_2}^{+'}/p_{H_2}^{3.5})(\alpha_{CH_3-l} p_{H_2}^{0.5} p_{H_2O}^2 - (k_M^{+'}/k'_{CO_2} k_M^{-'}) p_{CO_2} p_{H_2}^4)}{(DEN)^2},$$

$$R_{WGS} = \frac{(k_{WGS}^{+'}/p_{H_2})(p_{CO} p_{H_2O} - (1/K_{WGS}) p_{CO_2} p_{H_2})}{(DEN)^2}$$

with

$$\alpha_{CH_3-l} = \frac{(p_{H_2}^{0.5} + 3\kappa/p_{H_2}^{0.5} + \kappa) k_P^{+'} p_{C_3H_g} + 2k_E^{+'} p_{C_2H_6} + k_M^{+'} p_{CH_4} + (k_{CO}^{+'} k_M^{+'}/K'_{CO} k_M^{-'}) p_{CO} p_{H_2}^{0.5} + (k_{CO_2}^{+'} k_M^{+'}/K_{CO_2}^{-'} k_M^{-'}) p_{CO_2} p_{H_2}^{0.5}}{k_M^{-'} p_{H_2}^{0.5} + k_{CO}^{+'}(p_{H_2O}/p_{H_2}^2) + k_{CO_2}^{+'}(p_{H_2O}^2/p_{H_2}^3)}$$

and

$$DEN = 1 + \alpha_{CH_3-l} + K_{CHO-l}(p_{H_2O}/p_{H_2}^2)\alpha_{CH_3-l} + K_{CH_4} p_{CH_4} + K_{CO} p_{CO} + K_{CO_2} p_{CO_2} + K_{H_2}^{0.5} p_{H_2}^{0.5} + K_{H_2O} \frac{p_{H_2O}}{p_{H_2}}$$

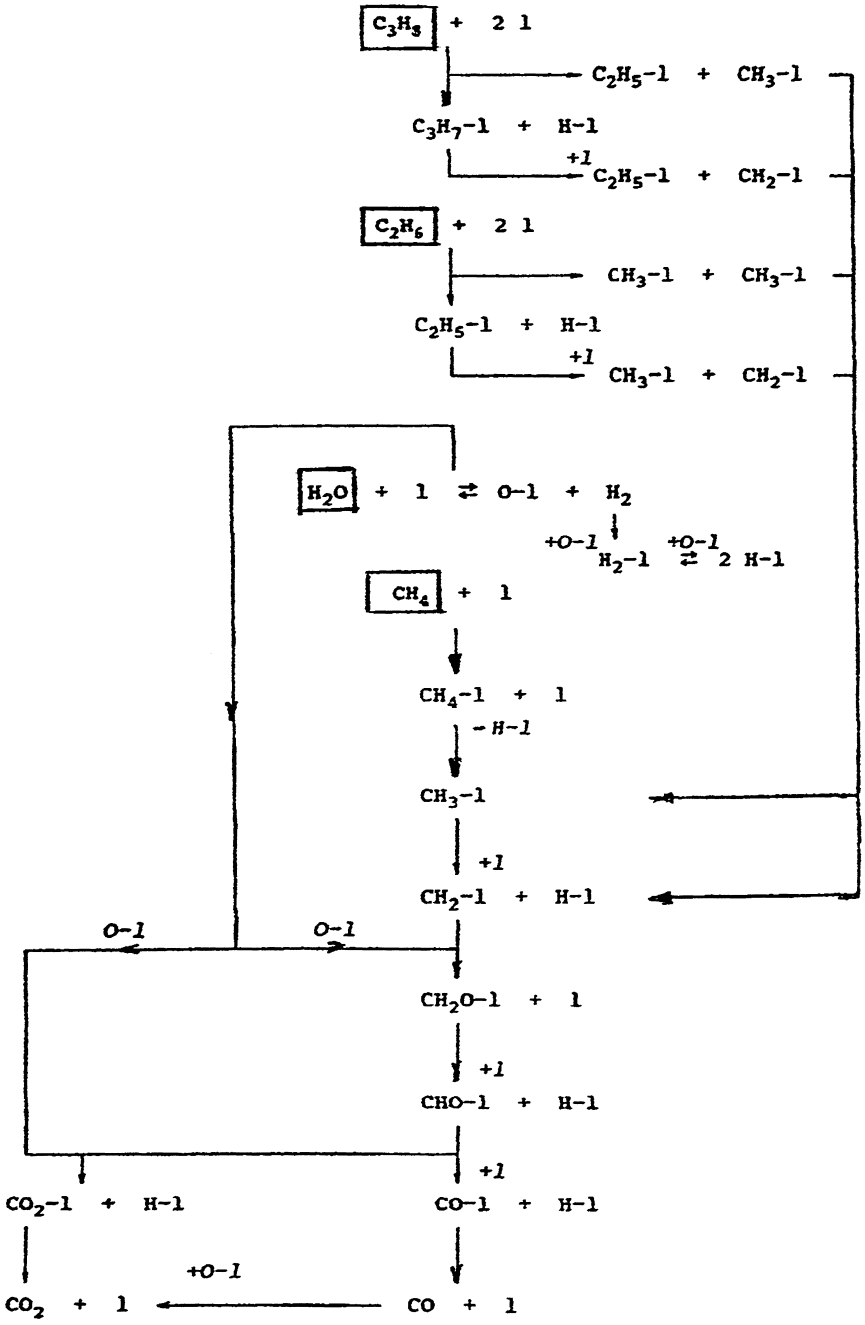

Fig. 1. Detailed reaction scheme for steam- and CO_2-reforming of ethane:methane mixtures [1,3].

$C_3H_8 + 2l \rightarrow C_2H_5\text{-}l + CH_3\text{-}l$	rds; k_{P1}^+
$C_3H_8 + 2l \rightleftarrows C_3H_7\text{-}l + H\text{-}l$	rds; k_{P2}^+, k_{P2}^-
$C_3H_7\text{-}l + l \rightarrow C_2H_5\text{-}l + CH_2\text{-}l$	rds; k_{P3}^+
$C_2H_6 + 2l \rightarrow 2\,CH_3\text{-}l$	rds; k_{E1}^+
$C_2H_6 + 2l \rightleftarrows C_2H_5\text{-}l + H\text{-}l$	rds; k_{E2}^+, k_{E2}^-
$C_2H_5\text{-}l + l \rightarrow CH_3\text{-}l + CH_2\text{-}l$	rds; k_{E3}^+
$CH_4 + l \rightleftarrows CH_4\text{-}l$	K_{CH4}
$CH_4\text{-}l + l \rightleftarrows CH_3\text{-}l + H\text{-}l$	rds; k_M^+, k_M^-
$CH_3\text{-}l + l \rightleftarrows CH_2\text{-}l + H\text{-}l$	K_3
$CH_2\text{-}l + O\text{-}l \rightleftarrows CH_2O\text{-}l + H\text{-}l$	K_6
$CH_2O\text{-}l + l \rightleftarrows CHO\text{-}l + H\text{-}l$	K_7
$CHO\text{-}l + l \rightleftarrows CO\text{-}l + H\text{-}l$	rds; k_{CO}^+, k_{CO}^-
$CO\text{-}l \rightleftarrows CO + l$	$1/K_{CO}$
$CHO\text{-}l + O\text{-}l \rightleftarrows CO_2\text{-}l + H\text{-}l$	rds; k_{CO2}^+, k_{CO2}^-
$CO_2\text{-}l \rightleftarrows CO_2 + l$	$1/K_{CO2}$
$CO\text{-}l + O\text{-}l \rightleftarrows CO_2\text{-}l + l$	rds; k_{WGS}^+, k_{WGS}^-
$H_2O + l \rightleftarrows O\text{-}l + H_2$	K_{H2O}
$2\,H\text{-}l \rightleftarrows H_2 + 2l$	$1/K_{H2}$

Fig. 2. Elementary steps in the steam- and CO_2-reforming of natural gas.

Fig. 3 shows the rate and adsorption equilibrium coefficients in an Arrhenius/van t'Hoff plot for the steam- and CO_2-reforming of methane. The values of the rate coefficients given here are intrinsic, i.e. they are determined from experiments with crushed catalyst to avoid diffusional limitations.

3. Diffusional limitations

As mentioned already the rate equations given here are intrinsic. In the present approach the diffusional limitations are introduced through the modeling, using appropriate characterization of the structure of the catalyst particle and accurate equations for the molecular- and Knudsen-diffusivities, rather than measuring the rates on the full size catalyst particle. The latter approach suffers from the unknown hydrodynamic pattern in a lab scale reactor with small internal diameter containing only one or two particles in a cross section.

The continuity equations for CH_4 and CO_2 inside the catalyst pellets can be written

$$\frac{1}{\xi^2 d\xi}\left(D_{e,CO_2}\xi^2\frac{dp_{s,CO_2}}{d\xi}\right) = 10^{-5}RT\cdot R_P^2\cdot r'_{CO_2}(P_s)\rho_s,$$

$$\frac{1}{\xi^2 d\xi}\left(D_{e,CH_4}\xi^2\frac{dp_{s,CH_4}}{d\xi}\right) = 10^{-5}RT\cdot R_P^2\cdot r'_{CH_4}(P_s)\rho_s$$

with $P_s = (p_{s,CO_2}; p_{s,CH_4}; p_{s,H_2}; p_{s,CO}; p_{s,H_2O})^T$

Boundary conditions:

$$\frac{dp_{s,CO_2}}{d\xi} = \frac{dp_{s,CH_4}}{d\xi} = 0 \text{ at } \xi = 0,$$

$$p_{s,CO_2} = p_{CO_2},\ p_{s,CH_4} = p_{CH_4} \text{ at } \xi = 1$$

The profiles of the dependent components are obtained from the algebraic equations

$$p_{s,CO} - p_{CO} = \left(\frac{D_{e,CO_2}}{D_{e,CO}}\right)(p_{CO_2} - p_{s,CO_2}) - \left(\frac{D_{e,CH_4}}{D_{e,CO}}\right)(p_{s,CH_4} - p_{CH_4}),$$

$$p_{s,H_2O} - p_{H_2O} = \left(\frac{D_{e,CO_2}}{D_{e,H_2O}}\right)(p_{CO_2} - P_{s,CO_2}) + \left(\frac{D_{e,CH_4}}{D_{e,H_2O}}\right)(p_{s,CH_4} - p_{CH_4}),$$

$$p_{s,H_2} - p_{H_2} = \left(\frac{D_{e,CO_2}}{D_{H_2}}\right)(p_{s,CO_2} - p_{CO_2}) - \left(\frac{3D_{e,CH_4}}{D_{e,H_2}}\right)(p_{s,CH_4} - p_{CH_4}) \quad (5)$$

The effective diffusivities entering in the above equations are given by

$$D_{eA}(r_i) = \frac{\varepsilon_s}{\tau}\left(\frac{1}{D_{mA}} + \frac{1}{D_{K,A}(r_i)}\right)^{-1} \quad (6)$$

where D_m and D_K are the molecular and Knudsen diffusivity of component i, the symbol ε represents the porosity of the particle and τ the tortuosity factor, expressing the topology of the pore network.

The pore size distribution was measured using standard commercial equipment and τ was obtained from the fitting of data on the reverse of the water gas shift; carried out in a tubular reactor with internal diameter of 1.07×10^{-2} m and containing particles with a size of 1.1×10^{-3} m. A value of 3.54 was obtained for τ.

Profiles of partial pressures in a catalyst particle at 7 m from the inlet of a methane steam reformer are

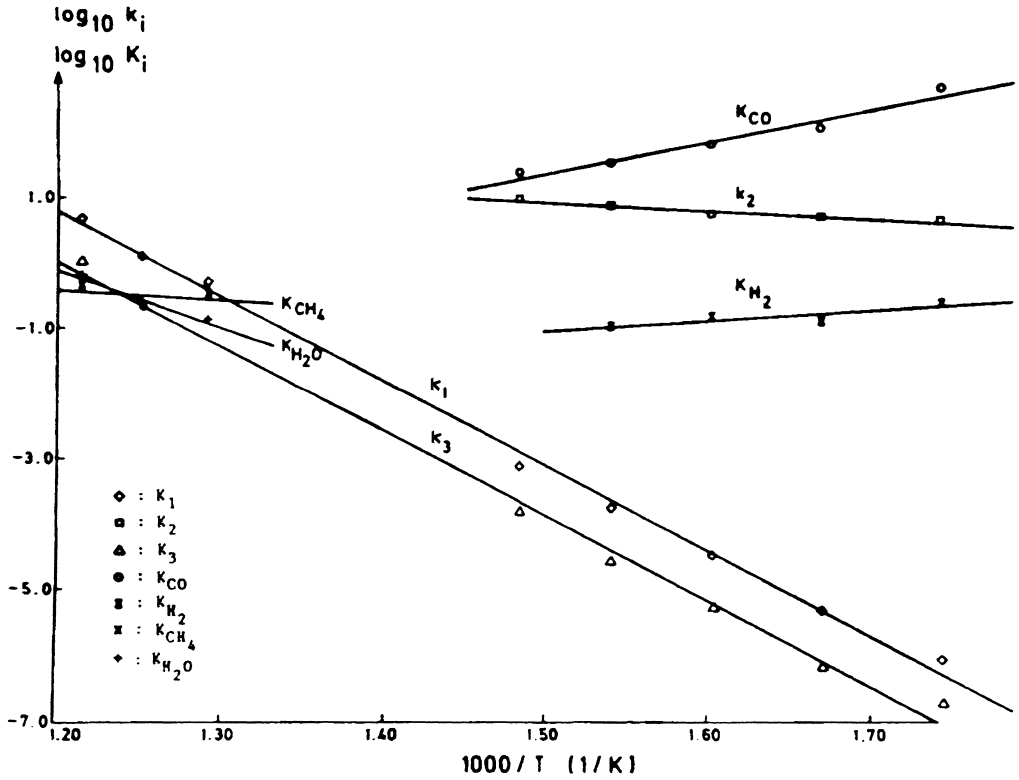

Fig. 3. Arrhenius- and van t'Hoff-diagram for the rate-coefficients and adsorption–equilibrium constants for methane–steam reforming [1].

given in Fig. 4. The variation of the partial pressures is limited to a very thin zone close to the surface with a thickness of only 5×10^{-5} m. It is obvious that it is not necessary to produce catalysts with a Ni-content which is uniform through the whole particle.

The observed rate is given by

$$r_{\text{obs}} = \int r_j(p_s)\frac{\mathrm{d}v}{S} \tag{7}$$

The effectiveness factor can be calculated from the profiles of Fig.4 through the Eq. (8):

$$\eta_i = \frac{\int_0^v r_i(P_s)\,\mathrm{d}V}{r_i(P_s^s)V} \tag{8}$$

The η_j for the CO- and CO_2-formation are very low-of the order of 0.03. This is an incentive to use very small particles, but to avoid excessive pressure drop fluidized or riser beds are then required.

4. Coke formation

Carbon deposition requires special attention in steam reforming since it leads to deactivation and even disintegration of the catalyst.

Three reactions are considered as potential sources of coking:

methane cracking; $CH_4 = C + 2H_2$ (9)

Boudouard reaction $2CO = C + CO_2$ (10)

CO-reduction $CO + H_2 = C + H_2O$ (11)

Untill now thermodynamic criteria based upon the affinity-concept have been used to check the possibility of coke formation:

$$V_i = \frac{\frac{\Pi_p p_p^{\alpha_p}}{\Pi_z p_z^{\alpha_z}}}{K_i} \tag{12}$$

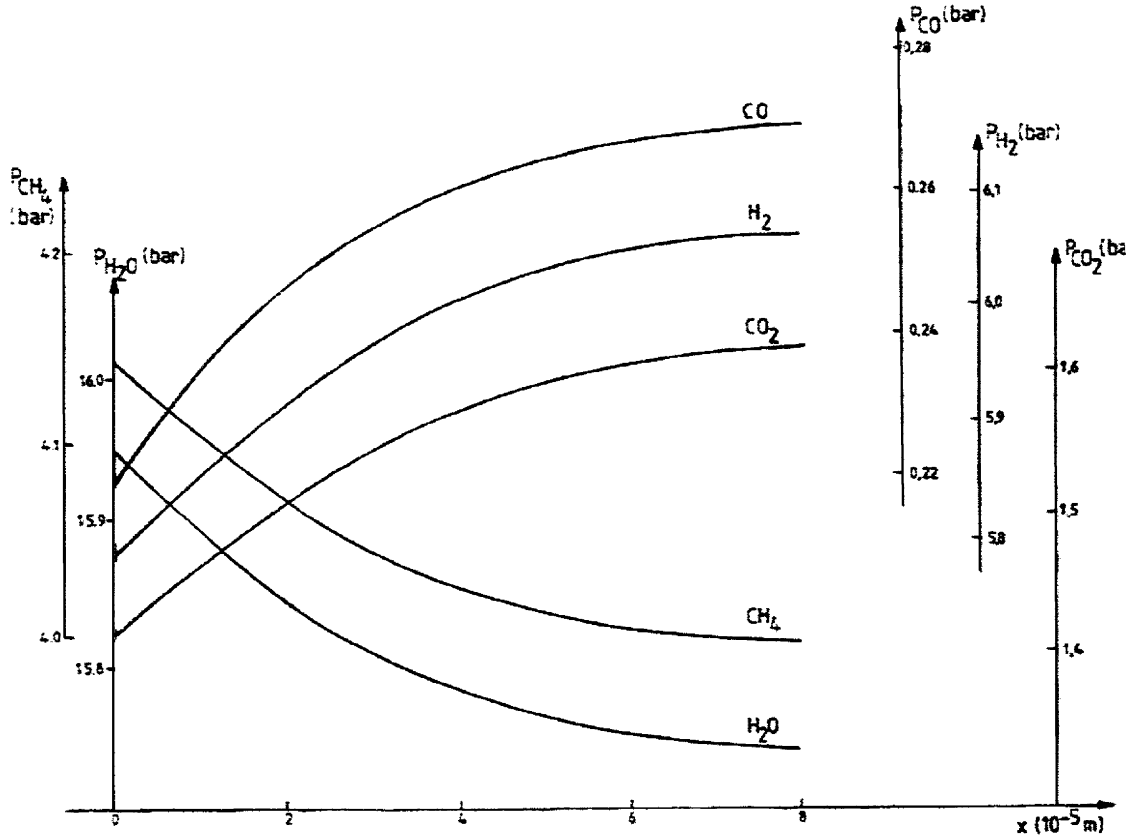

Fig. 4. Partial pressure profiles in a catalyst particle at $z = 7.00$ m from the inlet of a methane steam reformer [2].

where K_i is the equilibrium constant of reaction i. The reaction proceeds from left to right when $V_i < 1$, from right to left when $V_i > 1$. The affinity for C-formation in a steam reformer will be shown in the section on reactor simulation of this paper. The affinity for CH_4-cracking decreases from the surface to the center of the particle. If there is no affinity for CH_4-cracking in the bulk of the fluid there will be no affinity for C-formation inside the particle. In the center, where the reacting components have reached equilibrium, all the affinities are equal. In those situations where there is affinity for C-formation by CH_4-cracking but also for the gasification of carbon by steam and CO_2 a kinetic approach is required to evaluate the potential for coke-formation. Such an approach was developed by Snoeck and Froment (4,5). The experimental data on C-formation and gasification were obtained in an electrobalance unit, operated in the differential mode. The catalyst was crushed so as to measure intrinsic rates. Carbon-filament (whisker)-formation was observed and was accounted for in the modeling. All the possible elementary step schemes for methane-cracking are shown in Fig. 5.

All together there are 36 possible pathways from methane to adsorbed carbon. Methane can adsorb molecularly or dissociatively and further undergo stepwise or saltatory dehydrogenation. Each step can be rate determining. This leads to 80 possible rate equations. The primary reaction product, adsorbed carbon does not desorb into the gas phase but dissolves in the Ni, diffuses through it and precipitates at the rear of the nickel crystallite with formation of a growing carbon-filament. The finally retained model contains the following steps, also shown in Fig. 5.

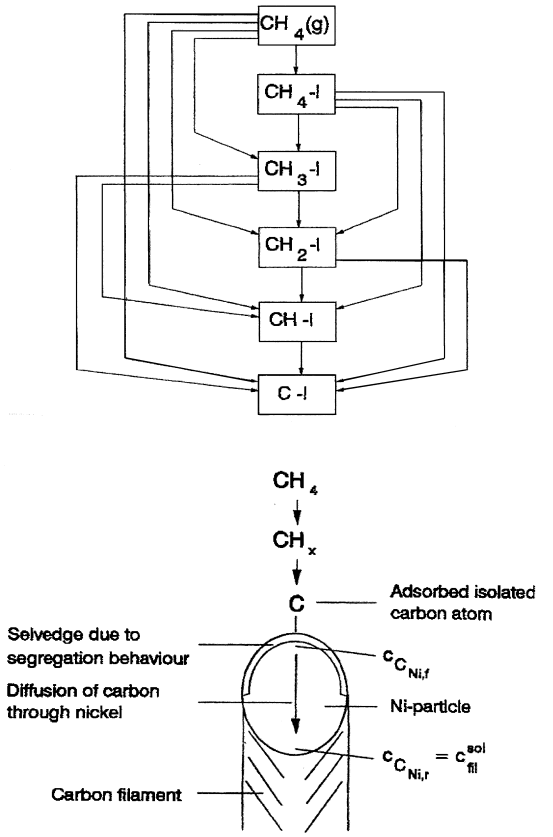

Fig. 5. Elementary steps of methane-cracking on a Ni-alumina catalyst [4].

Surface reaction :

$$\begin{aligned}
CH_4 + l &\rightleftarrows CH_4 - l && K_{CH_4}\\
CH_4 - l + l &\rightleftarrows CH_3 - l + H - l && \frac{\text{rds}}{k_M^+ \& k_M^-}\\
CH_3 - l + l &\rightleftarrows CH_2 - l + H - l && K_3 l\\
CH_2 l + l &\rightleftarrows CH - l + H - l && K_4 l \rightarrow K_r\\
CH - l + l &\rightleftarrows C - l + H - l && K_5 l\\
2H - l &\rightleftarrows H_2 + 2l && \frac{1}{K_H}
\end{aligned}$$

Dissolution/segregation:

$$C - l \rightleftarrows C_{Ni,f} + l \quad \frac{1}{K_C}$$

Diffusion of carbon through nickel:

$$C_{Ni,f} \Rightarrow C_{Ni,r}$$

Precipitation/dissolution of carbon:

$$C_{Ni,r} \rightleftarrows C_w K_w \tag{13}$$

When the surface concentrations of H-l; CH-l and CH_2-l are neglibly small the rate equation for the surface reaction can be written in a simplified way as

$$r_{C,M} = \frac{k_M^+ \cdot K_{CH_4} \cdot p_{CH_4} - (k_M^{-'}/K_r') \cdot K_C \cdot c_{C,Ni,f} \cdot p_{H_2}^2}{(1 + K_C \cdot c_{C,Ni,f} + (1/k_r') \cdot K_C \cdot c_{C,Ni,f} \cdot p_{H_2}^{3/2} + K_{CH_4} \cdot p_{CH_4})^2} \tag{14}$$

$c_{C,Ni,f}$ is not accessible and is eliminated by combining the rate equation for the surface reaction with the rate equation for the diffusion of carbon through the Ni-particle

$$r_{C,diff} = \frac{D_{C,Ni}}{d_a} \cdot (c_{C,Ni,f} - c_{C,Ni,r}) \cdot a_{Ni}. \tag{15}$$

The concentration of C dissolved in Ni at the support side of the particle, $c_{C,Ni,r}$, equals the saturation concentration of filamentous carbon when the supersaturation is very small during steady state filament growth. At steady state $r_{CM} = r_{C,diff}$. Eliminating the concentration of carbon at the gas side surface of the Ni-particle, $c_{C,Ni,f}$, leads to an implicit equation for the rate of carbon formation by methane cracking which is represented in a slightly simplified explicit form by the following equation

$$r_{CM} = \frac{k_M^+ \cdot K_{CH_4} \cdot p_{CH_4} - (k_M^{-'}/k_r'') \cdot p_{H_2}^2}{(1 + (1/k_r'') \cdot p_{H_2}^{3/2} + K_{CH_4} \cdot p_{CH_4})^2}. \tag{16}$$

This equation accounts for all the steps in methane cracking on a Ni-catalyst as described by the set of Eq. (13). It is clear that the methane cracking process should not be dealt with as a simple equilibrium reaction. Notice that the parameters in (16) are such that r_{CM} decreases as p_{H_2} increases and p_{CH_4} decreases.

The approach outlined above was extended by Snoeck et al. [8,9] to account also for carbon formation from CO through the Boudouard reaction and for gasification by H_2 or by adsorbed oxygen out of H_2O or CO_2. This enables to simulate the net rate of C-formation in a steam- or CO_2-reformer. The

elementary steps are

$$
\begin{aligned}
&CH_4 + l \rightleftarrows CH_4 - l && K_{CH_4},\\
&CH_4 - l + l \rightleftarrows CH_3 - l + H - l && \text{rds}\ \frac{l}{k'_M \& k_M}\\
&CH_3 - l + 3l \rightleftarrows C - l + 3H - l && K_r\\
&H_2 + 2l \rightleftarrows 2H - l && K_H,\\
&C - l \rightleftarrows C_{Ni,f} + l && \frac{1}{K_C}\\
&CO_2 + 2l \rightleftarrows O - l + CO - l && \\
&\quad \frac{1}{K_{O,CO_2}}; k^+_{O,CO_2} \& k^-_{O,CO_2} && \\
&CO - l \rightleftarrows CO + l && \frac{1}{K_{CO}}\\
&H_2O + l \rightleftarrows O - l + H_2 && \frac{1}{K_{O,H_2O}; k^+_{O,H_2O} \& k^-_{O,H_2O}}\\
&C - l + O - l \rightleftarrows CO - l + l && \text{rds}\frac{2}{k^+_O \& k^-_O} \qquad (17)
\end{aligned}
$$

The equation for the net rate of carbon formation is

$$
r_{C,net} = \frac{\begin{array}{c}(k^+_M \cdot K_{CH_4} \cdot p_{CH_4} - (k^{-'}_M / k^{''}_r) \cdot p^2_{H_2})\\ +(k^-_O \cdot K_{CO} \cdot p_{CO} - k^{+'}_O \cdot \alpha_{O-l})\end{array}}{\begin{array}{c}(1 + K_{CO} \cdot p_{CO} + K_{CH_4} \cdot p_{CH_4}\\ +(1/K''_r) \cdot p^{3/2}_{H_2} + \alpha_{O-l})^2\end{array}} \qquad (18)
$$

The first term between brackets in the numerator describes the carbon formation from methane and its gasification by hydrogen, the second term the carbon formation from carbon monoxide and the gasification by steam and carbon dioxide: Since the net rate of carbon formation from steam reforming mixtures is very low it was assumed in this derivation that the diffusivity of carbon in the nickel is sufficiently high to maintain a negligible carbon concentration gradient over the nickel particle.

Fig. 6 shows the influence of the partial pressures of the components of the reaction mixture. The agreement between the experimental and the calculated date for $r_{C,net}$ is good, so that (18) will be used in the simulation of steam- and CO_2-reformers.

5. Simulation of an industrial steam reformer.

The one-dimensional heterogeneous reactor model accounting for intraparticle diffusion limitations can be written according to Froment and Bischoff [10].

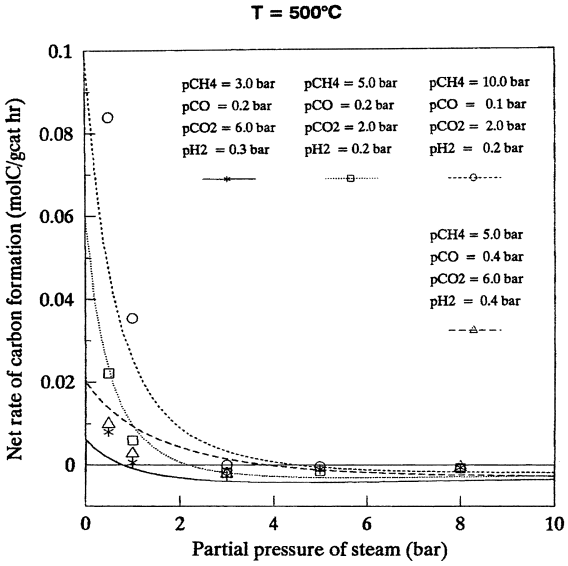

Fig. 6. Carbon formation and gasification from steam- and CO_2-reforming mixtures. $T = 500°C$.

Continuity equations for methane and CO_2:

$$\frac{dx_{CH_4}}{dz} = \Omega \frac{\rho_B - \eta_{CH_4} \cdot R_{CH_4}}{F^0_{CH_4}},$$

$$\frac{dx_{CO_2}}{dz} = -\Omega \frac{\rho_B - \eta_{CO_2} \cdot R_{CO_2}}{F^0_{CH_4}}$$

Energy equation:

$$\frac{dT}{dz} = \frac{1}{c_p \cdot \rho_g \cdot u_s} \left[\rho_B \cdot \left(\sum (-\Delta H_i) r_i \eta_i \right) - 4 \frac{Q}{d_{t,i}} \right]$$

Momentum equation:

$$\frac{dp_t}{dz} = f \cdot \frac{\rho_g \cdot u^2_s}{g \cdot d_p}$$

with the following boundary conditions

$$x_{CH_4} = x_{CO_2} = 0; \quad T = T_0; \quad p_t = (p_t)_0 \ \text{at}\ z = 0$$

The gas film resistance is not considered. It has been shown by De Deken et al [12] to be negligible. On the other hand the diffusional transport inside the catalyst particle, expressed by the set of Eq. (5), has to be accounted for in each point of the reactor.

The furnace is gas fired by means of radiant side-wall burners or by long flame burners located in the roof or bottom of the furnace. The operation of the

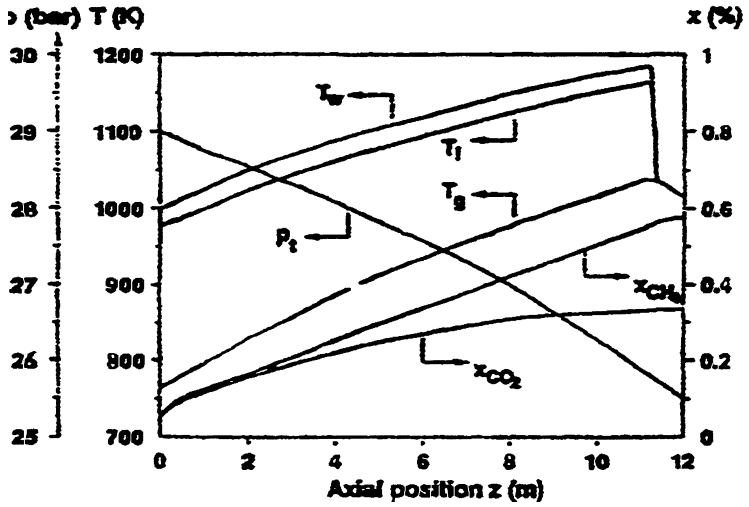

Fig. 7. Profiles of methane conversion (x_{CH_4}), gas temperature (T_g), internal (T_i) and external (T_w) tube skin temperatures and total pressure (p_t) in an industrial steam refomier [2].

furnace and reactor tubes has been modeled and simulated by Plehiers and Froment [11] Typical external tube-skin temperatures derived from this model for a side-wall fired furnace were used in the present work.

The profile of the total methane-conversion into CO_2, the process gas temperature, the internal and external tube-skin temperature and the total pressure in an industrial methane steam reformer are given in Fig. 7. The tube exit is located outside the furnace proper and is considered to operate adiabatically.

CO_2-reforming can also be simulated with the present model Table 1 shows various input values for the ratios H_2O/CH_4 and CO_2/CH_4 and also the simulated temperature and H_2/CO ratio at the exit. For a given methane inlet partial pressure and heat input the total methane conversion is reduced from 72% when $H_2O/CH_4 = 2.0$ to 69% when this ratio equals 1.3 and $CO_2/CH_4 = 0.7$, but the H_2/CO ratio is lowered to a value appropriate for methanol synthesis. A crucial aspect in reforming is the amount of steam that can be replaced by CO_2 without running into carbon formation. Fig. 8, based upon affinities, shows in the first place that only methane cracking is critical in this respect, but also that a model ignoring

Table 1
H_2O/CH_4- and CO_2/CH_4-feed ratios, H_2/CO ratio and process gas temperature at the reactor outlet for the simulations of Fig. 9.

H_2O/CH_4	CO_2/CH_4	T_{exit} (°C)	H_2/CO at exit
3	0	855.2	5.32
2	0	855.2	4.60
1	0	861.4	3.76
1.5	0.5	844.3	2.36
1.3	0.7	844.2	1.98

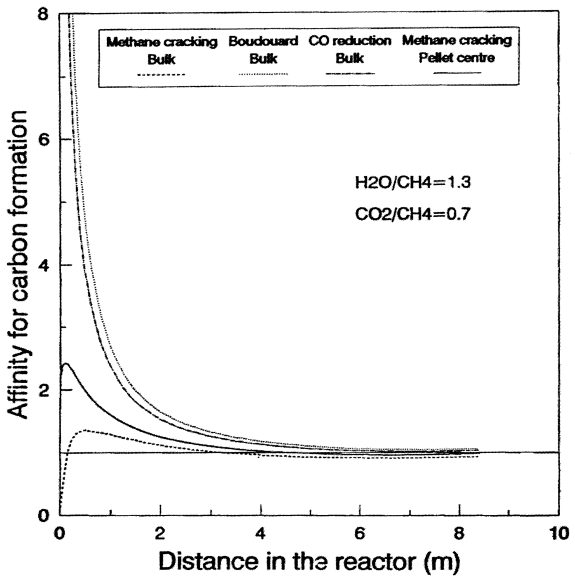

Fig. 8. Affinity for carbon formation in the gas-phase and in the particle center along a steam-CO_2-reformer.

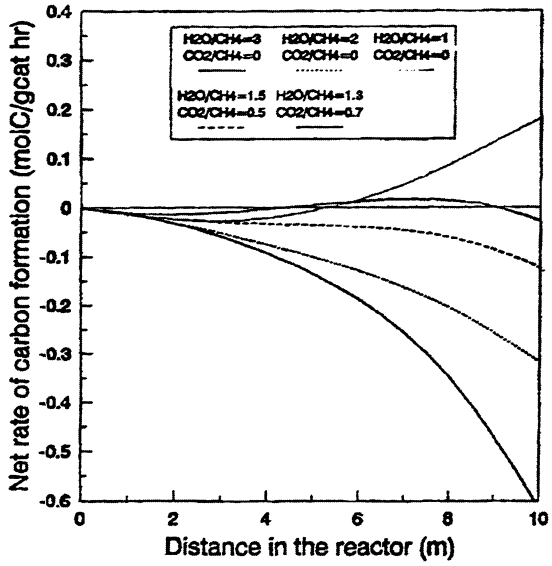

Fig. 9. Net rate of carbon formation as a function of reactor length in a steam-CO_2-reformer for various feed compositions.

internal diffusional limitations i.e. differences in partial pressures at the surface and in the center of the catalyst particle, can lead to erroneous conclusions. It follows from the partial pressure values in the bulk or at the particle surface that the case $H_2O/CH_4 = 1.3$ and $CO_2/CH_4 = 0.7$ exhibits affinity for coke formation by methane cracking from 3 m onwards. This is confirmed by Fig. 9 showing the net rate of carbon formation, based upon the kinetic equations [16] and predicting coke formation between 4 and 9 m. The worst case is that with the ratio $H_2O/CH_4 = 1.0$, i.e. with the highest partial pressure of methane.

6. Conclusion

The modeling approach applied here to the production of synthesis gas by reforming is a powerful tool for the analysis, simulation and design of this process. It provides a better insight into the role of the numerous variables and into their interaction. Crucial aspects, like the substitution of a fraction of the steam by CO_2 and/or the risk of carbon formation, can be investigated in a more comprehensive way than by a conventional experimental program. The model is of particular interest for the conceptual design of new reactor configurations and, given its fundamental kinetic basis, for the development of more performing new catalysts.

References

[1] D.L. Trimm, Catal. Rev.-Sci. Eng. 16 (1977) 155.
[2] C.H. Bartholomew, Catal. Rev.-Sci. Eng. 24 (1982) 67.
[3] J. Rostrup-Nielsen, Catalysis Science and Technology, Vol. 5, Catalytic Steam Reforming, Springer, New York, 1984.
[4] M.V. Twigg, Catalyst Handbook, Wolfe Publishing Ltd., 1989.
[5] J. Xu, G.F. Froment, Methane steam reforming, methanation and water gas shift. 1. Intrinsic kinetics, AIChE. J. 35 (1) (1989) 88–96.
[6] J. Xu, G.F. Froment, Methane steam reforming. II. Diffusional limitations and reactor simulation, AIChE. J. 35 (1) (1989) 97–103.
[7] F. Vereecke, G.F. Froment, unpublished.
[8] J.W. Snoeck, G.F. Froment, M. Fowles, Kinetic study of the carbon-filament formation by methane -cracking on a nickel-catalyst, J. Catal. 169 (1997) 250–262.
[9] J.W. Snoeck, G.F. Froment, M. Fowles, Filamentous carbon formation and gasification. Thermodynamics; driving force, nucleation and steady state growth, J. Catal. 169 (1997) 240–249.
[10] G.F. Froment, K.-B. Bischoff, Chemical Reactor Analysis and Design, 2nd Edition, Wiley, New York, 1990.
[11] P.M. Plehiers, G.F. Froment, Coupled simulation of heat transfer and reaction in a steam reforming furnace, Chem. Eng. Technol. 12 (1989) 20–26.
[12] J.C. De Deken, E.F. Devos, G.F. Froment, Steam reforming of natural gas: intrinsic kinetics, diffusional influences and reactor design, ACS Symp. Ser. 196, Chem. React. Eng., 1981.